Chapter 4 – SPONTANEOUS RADIO FREQUENCY EMISSIONS FROM NATURAL AURORA

J. LaBelle
Dartmouth College, Department of Physics and Astronomy, Hanover, NH, USA

June 9, 2006

Abstract. At high latitudes, suitably sensitive radio experiments tuned below 5 MHz detect up to three types of spontaneous radio emissions from the Earth's ionosphere. In recent years, ground-based and rocket-borne experiments have provided strong evidence for theoretical explanations of the generation mechanism of some of these emissions, but others remain unexplained. Achieving a thorough understanding of these ionospheric emissions, accessible to ground-based experiments, will not only bring a deeper understanding of Earth's radio environment and the interactions between waves and particles in the ionosphere but also shed light on similar spontaneous emissions occurring elsewhere in Earth's environment as well as other planetary and stellar atmospheres.

1. Introduction

While it cannot be excluded that radio frequency emissions might occur in all ionospheric regions, only from the auroral ionosphere, at magnetic latitudes from 65 to 75 degrees, are such emissions regularly observed and extensively documented. The auroral region uniquely contains the energy source for such emissions, which is the highly nonthermal electron distribution functions associated with the northern and southern lights phenomena.

As discussed in the Introduction, the auroral ionosphere is dominated by processes imposed upon it from the magnetosphere. In particular, magnetospheric processes drive field-aligned currents into and out of the ionosphere that must be closed across the ionospheric plasma. In the region where an upward current is imposed, this current must be carried by downward electrons. Because these are scarce at high altitudes, a field-aligned electric field develops, typically at altitudes of several thousand kilometers, to accelerate these electrons to energies of 1–10 keV, enabling them to carry the required current. As a result, at ionospheric altitudes the distribution of electrons not only includes the cold (0.1 eV), approximately isotropic ionospheric plasma, but also includes the 1–10 keV beam, which by the time it reaches the ionosphere has been scattered into a ring distribution. Electrons with velocities directed too nearly parallel to the magnetic field are lost in the atmosphere and not backscattered, so the energetic distribution actually resembles a ring with a loss cone removed from it in the upward direction parallel to the magnetic field; this distribution is sometimes called a “horseshoe.” In addition to the cold plasma and the energetic beam, there is a background of warm secondary scattered particles generated by impact ionization. Detailed features result because some electrons are trapped between the converging magnetic field below and the downward-accelerating electric field above. This auroral electron distribution function was first described in a classic paper by Chiu and Schulz (1978). Taken together, these populations of electrons comprise a highly non-Maxwellian distribution, containing ample free energy. In its attempt to relax to a thermal distribution, the plasma excites both electrostatic and electromagnetic waves; the latter may propagate long distances as radio emissions, and the former may mode-convert to electromagnetic waves observable at long distances.

Other regions of the aurora may also provide sources of spontaneous emissions. In the region where a downward field-aligned current is imposed on the ionosphere, electrons are extracted and the electron density becomes depleted in the ionosphere; eventually a dearth of ionospheric electrons leads to formation of electric fields parallel to the magnetic field accelerating electrons upward in this region. In the dayside auroral latitudes near noon local time, the “cusp” feature of the geomagnetic field allows direct access of solar wind particles which provide another population of electrons. In other

auroral regions, time dependent field-aligned currents imposed by magnetospheric activity or magnetosphere-ionosphere interactions are carried by Alfvén waves which accelerate electrons locally, causing bursts of electrons directed along the magnetic field line with a broad range energies from a fraction of an eV to hundreds of eV. The electron distributions in these regions is different from that described above but is also highly non-Maxwellian, containing free energy for spontaneous emissions.

At mid- and low-latitudes, the ionosphere contains non-Maxwellian electron distributions as well, resulting for example from photo-ionization. However, the non-Maxwellian features of the auroral ionosphere, described above, are much more extreme. For this reason, the auroral ionosphere generates multiple types of spontaneous emissions which are easy to observe, whereas spontaneous emissions have not been reported from the other regions. Section 2 review the spontaneous emissions from the auroral ionosphere which are observable at ground level.

2. Emissions Observable at Ground-Level

Figure 1 shows 0-5 MHz signals recorded at Arviat, Nunavut, on April 24, 1995, using a magnetic loop antenna and a 10-kHz bandwidth stepped-frequency receiver. (See Weatherwax et al. (1995) for a description of the receiver and sensor.) This spectrogram covers 0-5 MHz on the vertical axis, 0620–0720 UT on the horizontal axis, and the gray scale represents the power spectral density ranging from 5 nV/m$\sqrt{\text{Hz}}$ (white level) to 500 nV/m$\sqrt{\text{Hz}}$ (black level). The spectrogram covers an hour around local magnetic midnight (0635 UT) which is the most favorable time for observing spontaneous emissions from the aurora. On such a spectrogram, man-made signals, which are typically constant-frequency, stand out as horizontal dark bands. The abundance of such signals at 550–1600 kHz corresponds to the AM broadcast band (since extended to 1700 kHz). However, three types of signals stand out as distinct from the man-made signals. These represent the three types of radio emissions of auroral origin: Auroral Hiss, a broad-band impulsive emission extending from VLF up to about 1 MHz; Auroral MF-burst, a broad-band impulsive emission often coincident with hiss which occurs in the range 1500–4500 kHz; and Auroral Roar, a narrow-band emission which occurs near 3 MHz and 4.5 MHz. (The 4.5 MHz emission is not shown in Figure 1.)

2.1. Auroral Roar Emissions

Figure 1 shows an example of an auroral roar emission occuring at 2.8–3.0 MHz, which is more or less continually present from 0625–0645 UT but becomes intermittent after that. A substorm onset occurs at 0652 UT,

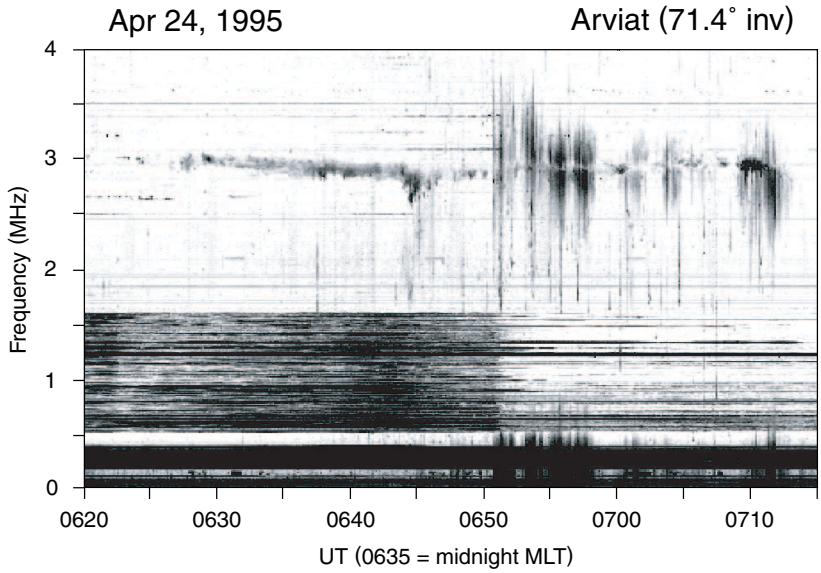

Figure 1. Auroral emissions recorded at Churchill, Manitoba (69.2° magnetic latitude) around the time of a substorm onset at 0652 UT on April, 24, 1995, showing the three types of spontaneous radio emissions generated in the auroral ionosphere and observable at ground-level: The narrowband emission centered at 2.9-3.0 MHz is auroral roar, the broadband emission at 1.5-3.8 MHz is auroral MF-burst, and the broadband emission extending up to 0.5-1.0 MHz is auroral hiss.

evidenced by the sudden decrease in the intensity of the AM broadcast signals reaching the receiver from distant sources. These broadcast signals are attenuated after the substorm onset due to absorption caused by the sudden and widespread ionization in the D-region associated with the enhanced substorm auroral activity. Typically auroral roar occurs continuously preceding the auroral substorm, sometimes for an hour or more rather than 20 minutes as in this example. After the substorm, the emission most likely continues but is probably screened from ground level by the enhanced D- and E-layer ionization. This hypothesis explains the intermittent nature of the emissions following substorm onset, but no suitably sensitive rocket- or satellite-borne experiment has yet confirmed it.

This auroral roar emission near 3 MHz is sometimes called "$2f_{ce}$-roar" because it matches twice the electron cycltron frequency ($2f_{ce}$) at F-region altitudes. This emission was first reported by Kellogg and Monson (1979). As mentioned above, there exists a second type of auroral roar which occurs

at 4.0–4.5 MHz, sometimes called "$3f_{ce}$-roar," first reported by Weatherwax et al. (1993). Observations from many observatories covering a range of magnetic latitudes show that the emission frequencies increase linearly with the magnitude of the geomagnetic field at the observatories, and the best linear fit implies that the emission frequency matches $2f_{ce}$ at about 275 km for the $2f_{ce}$-roar and matches $3f_{ce}$ at an equal or somewhat higher altitude for the $3f_{ce}$-roar (Hughes and LaBelle, 1998). At ground level the power spectral density of these emissions ranges up to 10^{-12} V^2/m^{2}Hz, which implies amplitudes of 10–100 μV/m. An isotropic radiator of 1–10 W at F-region altitudes suffices to explain such a weak signal level assuming no significant absorption. Hence, if the source size is reasonably large, greater than hundreds of meters as discussed below, the emission mechanism need not be very efficient, since 1-10 W is small compared to the auroral energy input of order 100 mW/m^2 over a source region of reasonable size. The polarization of the auroral roar has been measured and corresponds to O-mode propagation in the ionosphere (Shepherd et al., 1997).

Figure 2 illustrates the mechanism that has been put forward to explain auroral roar emissions. Altitude is shown on the vertical axis and frequency on the horizontal axis. The curves show "typical" profiles of the electron plasma frequency (f_{pe}) and the upper hybrid frequency (f_{uh}), which peak in the F-region at a few hundred kilometers altitude, and the electron cyclotron frequency and its first two harmonics which are decreasing functions of altitude. Depending on how large the electron density happens to be, locations may exist where f_{uh} matches $2f_{ce}$ or, under high-density conditions, $3f_{ce}$. These special locations are indicated by dots in Figure 2. Ample theoretical work (e.g., Kaufmann, 1980; Yoon et al., 1996, 1998a) shows that in the presence of the auroral electron distribution described above, electrostatic upper hybrid waves are favorably generated when the upper hybrid frequency matches a cyclotron harmonic. Hence, at the special locations indicated in Figure 2, one expects intense electrostatic waves in the presence of auroral electrons. If these electrostatic waves convert to electromagnetic waves, and if no blanketing E-region intervenes, they can penetrate to ground level to be observed as auroral roar emissions near 2.5–3.0 MHz and 4.0–4.5 MHz. (Gough and Urban (1983) first suggested this mechanism to explain the $2f_{ce}$ emission.) Direction finding observations of auroral roar at Sondrestrom, Greenland, show that the auroral roar signals, ray-traced into the ionospheric electron density profile observed with the incoherent scatter radar, reach points in the ionosphere where $f = 2f_{ce} = f_{uh}$ as predicted by this generation mechanism (Hughes and LaBelle, 2001b).

This mechanism predicts the existence of matching conditions at two special locations on the topside ionosphere, which should radiate electromagnetic waves upward into the topside ionosphere. Indeed, such topside emissions have been observed. From satellite data, James et al. (1974) reported

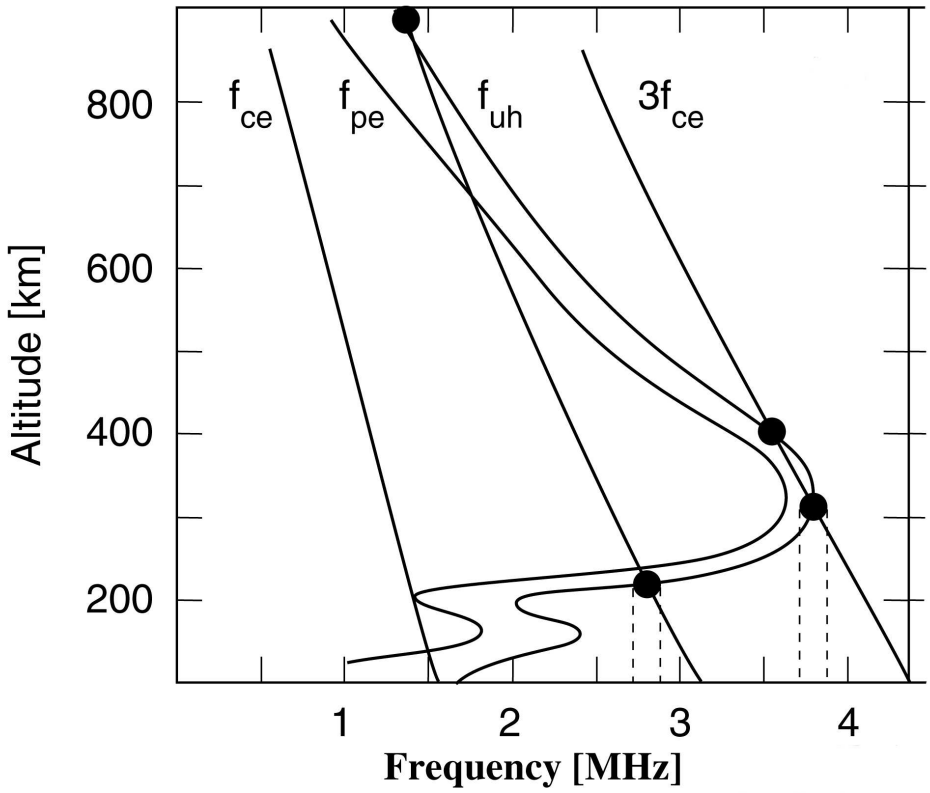

Figure 2. Typical profiles of critical resonance frequencies in the auroral ionosphere relevant to the generation mechanism of auroral roar emissions: The electron plasma and upper hybrid frequencies peak in the F-region, while the electron cyclotron frequency and its harmonics decrease with altitude. For sufficiently high F-region electron densities, locations exist where the upper hybrid frequency matches a cyclotron harmonic, indicated by dots in the figure. Intense electrostatic upper hybrid waves can be excited by the auroral electrons under these conditions. It they mode-convert to electromagnetic LO-modes, these can propagate to ground level and be observed as auroral roar.

emissions near 2- and 4-MHz in the topside ionosphere. These frequencies are somewhat below the corresponding frequencies observed at ground level, as expected from the model (Figure 2). Furthermore, from ray-tracing the observed signals into the topside ionospheric density profile determined by an ionospheric sounder on board the same spacecraft, James et al. (1974) concluded that the signals originated where f_{uh} matches $2f_{ce}$ and $3f_{ce}$. Benson and Wong (1987) analyzed many more of these topside 2- and 4-MHz signals observed with the ISIS-1 low-Earth orbit satellite, and Bale (1999)

reports one possible example observed at much greater distance from Earth with the WIND satellite.

However, the strongest evidence for the generation mechanism of auroral roar comes from sounding rocket observations. Long ago the Porcupine rocket experiment penetrated the F-region ionosphere and showed the prevalance of intense electrostatic waves occuring where $f_{uh} = 2f_{ce}$, both in the natural auroral ionosphere and in an plasma artificially enhanced by a Barium cloud explosion within the aurora [Carlson et al., unpublished manuscript, 1987]. More recently, the HIgh Bandwidth Auroral Rocket (HIBAR) encountered electrostatic waves occurring where $f_{uh} = 2f_{ce}$ near 300 km altitude in the natural auroral ionosphere (Samara et al., 2004). Unlike the earlier experiment, HIBAR included high-resolution measurements of the electron distribution function up to tens of keV with 30 ms cadence. Using these experimentally determined distribution functions, it was possible to calculate the growth rate of the Z-mode cyclotron maser instability at each frequency every 30 ms throughout the flight. The results show that strong growth rates, defined as e-folding times less than about 0.1 ms, occur only in the regions near the matching condition $f = f_{uh} = 2f_{ce}$ in which the enhanced electrostatic waves were observed; in other regions away from the matching condition, or in regions where the matching condition was met but no waves were observed, the calculated growth rate was small. This experiment directly confirms the generation of the electrostatic waves at the appropriate frequencies via Z-mode cyclotron maser in the auroral ionosphere.

The rocket experiments did not detect the mode-converted electromagnetic radiation. The HIBAR data thereby place an upper bound of about 3% on the mode conversion efficiency in the observed example. However, based on the observed upper hybrid wave intensities, mode conversion efficiency of only 1% is required to explain the intensity of the emissions observed at ground level. Future rocket experiments will include higher dynamic-range receivers in order to directly detect the mode converted waves and estimate the mode conversion efficiency. Little is known about the mode conversion mechanism. However, the auroral ionosphere is characterized by sharp density gradients which could result in refraction and direct linear conversion between electrostatic Langmuir-upper hybrid waves and LO-mode electromagnetic waves via the so-called Ellis window (see for example Yoon et al., 1998b). The auroral ionosphere also is highly irregular on many spatial scales, the condition for linear mode conversion via interaction with low frequency density irregularities as described by Bell and Ngo (1990). Nonlinear mode conversion mechanisms may also play a role.

For waves just below the matching condition $f_{uh} \approx 2f_{ce}$ the refractive index surface implies trapping in electron density enhancements. Both the Porcupine [Carlson et al., unpublished manuscript, 1987] and the HI-

BAR (Samara et al., 2004) rocket experiments show evidence for such wave trapping. Yoon et al. (2000) show that if the cross-sectional dimension of a field-aligned density enhancement is less than about 1 km, the upper hybrid waves generated at the matching conditions in such an inhomogeneous plasma would be discretized. Essentially, the wave trapping results in standing waves at certain selected eigenfrequencies for which the wave phase integrated between reflection points equals an odd-integer number of $\pi/2$. Yoon et al. (2000) calculate these eigenmodes using WKB approach and find two characteristic frequency gaps associated with the eigenmode structure, a relatively wide gap associated with the radial mode structure which might be of order 1 kHz for an 800-m density enhancement, for example, and a relatively narrower gap that might be of order 100 Hz for an 800-m density enhancement. The auroral ionosphere usually contains field-aligned irregularities of many different scales ranging from meters to kilometers. These irregularities might in some cases be generated by the very high frequency waves that are subsequently trapped in them, or they may more likely be pre-existing irregularities caused by electron impact ionization on small scales or filementation or other large scale instabilities such as $E \times B$ instability acting on density gradients. In any case, the conditions are often favorable to formation of upper hybrid waves with discrete frequency structure due to the inhomogeneous background plasma, and the mode converted electromagnetic waves would retain this frequency structure.

Figure 3 shows an example high-resolution spectrogram of the upper hybrid waves observed near the matching condition $f = f_{uh} = 2f_{ce}$ in the HIBAR rocket experiment (right panel) and a similar high-resolution spectrogram of auroral roar emissions observed at ground level. Strikingly both phenomena are characterized by fine structures. The auroral roar is composed of multiple discrete features separated by approximately 1 kHz and decreasing and increasing together in frequency (LaBelle et al., 1995; Shepherd et al., 1998). In Figure 3, as in many examples, two frequency separations are observed: a narrow band of hundreds of Hertz and a wider gap of several kHz. The rocket data show a similar structure for the upper hybrid waves. This structure matches qualitatively that predicted by the wave trapping theory of Yoon et al. (2000).

In summary, the auroral roar emission, first identified by Kellogg and Monson (1979), has become fairly well understood in broad outline. The evidence is pretty strong that Z-mode maser mechanism acting near the matching conditions $f = f_{uh} = 2f_{ce}$ can generate electrostatic waves with ~ 10 mV/m amplitudes in the F-region when an auroral electron beam is present. There is evidence that such waves are trapped in density enhancements as theory says should happen. There is also evidence, both in the direct measurements of upper hybrid waves and in the ground-level measurements of auroral roar, for fine frequency structure which qualitatively matches that predicted by theory

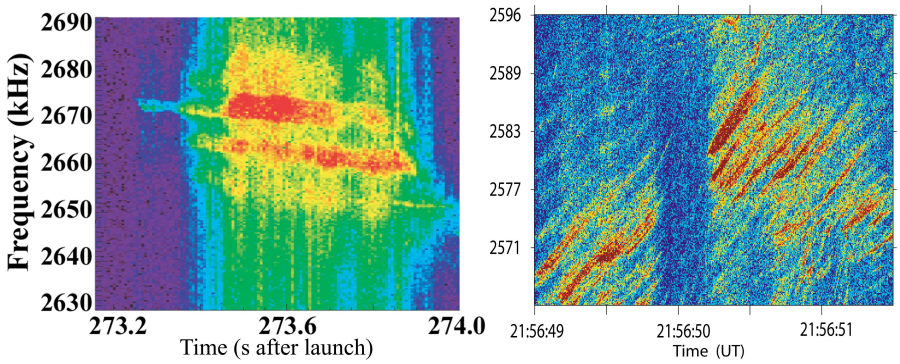

Figure 3. Fine structures characterizing upper hybrid waves and related electromagnetic auroral roar emissions: (a) Spectrogram of electric field fluctuations measured at an altitude of 277 km in the auroral ionosphere above Alaska, showing electrostatic upper hybrid waves with banded structure; (b) spectrogram of magnetic field fluctuations measured at ground level at South Pole, showing electromagnetic auroral roar with similar band structure.

of generation of discrete eigenmodes when the Z-mode maser acts in an inhomogeneous plasma characterized by field-aligned density irregularities with scale sizes of order tens to hundreds of meters. Quantitative comparison of the discrete eigenmode theory and the fine frequency structure observations is still lacking. The ingredient which is least well understood is the mode conversion mechanism, though a host of possibilities exist which could provide the required $\approx$ 1% mode-conversion efficiency. There are a host of other interesting time- and frequency-variations characterizing auroral roar emissions which defy precise explanation but may result from propagation effects or modulations of the causative auroral electron beams (e.g., Hughes and LaBelle, 2001a). Understanding these phenomena is the focus of current research. Possibly the auroral roar may prove to be a valuable means of remotely sensing ionospheric plasma processes in the aurora.

2.2. Auroral MF-burst Emissions

Figure 1 shows an example of an MF-burst emission occurring between 0652–0712 UT at 1.5–3.8 MHz. The emission thus coincides with the auroral substorm onset at 0652 UT; it is also coincident with impulsive auroral hiss at frequencies below 1 MHz, which is known to be associated with substorm onsets. The power spectral density of the MF-burst is in the range 10^{-13}–10^{-12} V^2/m^2Hz, comparable to that of auroral roar emission, but its bandwidth is ten times as great, implying that MF-burst requires an average source power of $\sim$ 100 W assuming it originates from an isotropic source at

F-region altitudes. However, high time-resolution measurements of LaBelle et al. (1997) suggest that auroral MF-burst consists of impulses of submillisecond duration, far faster than resolved in the spectrogram of Figure 2, and in this case the peak power required of an isotropic source might be as high as 1 kW (less if the source is beamed, of course). Polarization measurements show that the principal component of MF-burst, at frequencies above 1.5 MHz, is polarized consistent with O-mode propagation in the ionosphere (Shepherd et al., 1997).

The generation mechanism of auroral MF-burst remains unknown and little studied. The O-mode polarization suggests that MF-burst may consist of mode-conversion radiation similar to auroral roar. The striking correlation between MF-burst and auroral hiss, clearly visible in Figure 1, suggests a close connection between the generation mechanisms of these two emissions. (In general, the correlation between MF-burst and auroral hiss is not one-to-one; MF-burst occasionally occurs without corresponding hiss, and auroral hiss more commonly occurs unaccompanied by MF-burst.) Examining the dispersion relation for normal modes of a homogeneous plasma at frequencies associated with electrons, two modes stand out for which the index of refraction greatly exceeds unity: The whistler mode on its resonance cone, and the upper-hybrid/slow Z-mode. Even the relatively low energy (1-10 keV) electron beam has particle velocities exceeding the phase velocities of these modes, and hence the auroral electrons could Cherenkov radiate into each of these modes, yielding auroral hiss in the case of the whistler mode, and, following mode conversion, auroral MF-burst in the case of the upper-hybrid/slow Z-mode. If the two waves extracted energy from different parts of the electron distribution function, they could exist simultaneously because they would not compete directly for the same energy source; for example, if the hiss were generated via Landau resonance with parallel electrons whereas the upper hybrid/slow Z-modes were generated via resonance with perpendicular electrons. In this case, however, the interaction would probably need to take place over a range of altitudes in order to explain the broad frequency range of each emission, so the auroral electrons would need to have sufficient free energy to excite waves over a range of altitudes. Simultaneous ground-based MF-burst and incoherent scatter radar observations in Sondrestrom, Greenland, provide evidence that the upper frequency of MF-burst emissions is connected to the maximum plasma or upper hybrid frequency in the overlying ionosphere, as would be predicted if MF-burst is emitted at the local plasma or upper hybrid frequency over a range of altitudes. Alternative generation mechanisms have appeared in the literature: LaBelle et al. (1997) suggested excitation of Langmuir waves over a range of altitudes on the bottomside of the F-region, followed by mode conversion, and Sotnikov et al. (1996) suggested excitation of electron acoustic waves covering a broad band of frequencies up to the local plasma frequency, followed by mode conver-

sion. Quantitative work on these MF-burst generation mechanisms is not yet sufficient to enable experimental tests.

On occasion MF-burst emissions show interesting frequency structure that may provide further hints to its origin. Weatherwax et al. (1994) reported a gap in the MF-burst spectrum near $2f_{ce}$, especially in the case that auroral roar emissions occur around the same time at that frequency. Figure 1 shows an example of this $2f_{ce}$ frequency gap. Occasionally, MF-burst extends below 1.5 MHz, which is approximately the electron gyrofrequency. In these cases, the emission spectrum exhibits a sharp lower cutoff at about 1.5 MHz and a gap before resuming below that frequency. (LaBelle and Treumann (2002) show an example.) This latter feature could indicate that MF-burst consists of two modes in the ionosphere: LO-mode above f_{ce} and whistler mode below f_{ce}. The polarization of the component below f_{ce} has never been measured to confirm this hypothesis.

Auroral MF-burst is the least-known of the types of spontaneous emission from aurora. The first unambiguous ground-level observations of MF-burst occurred relatively recently (Weatherwax et al., 1994), although some earlier observations may have been related to MF-burst (for example, bursty emissions reported by Parthasarathy and Berkey (1964) and Kellogg and Monson (1979).) MF-burst emissions typically last only a few minutes at substorm onset, and this short duration makes it impossible to plan a rocket launch into MF-burst. (The example in Figure 1 which lasts 20 minutes is unusual in this regard.) Recently, Burchill and Pfaff (2005) reported broadband impulsive emissions in the MF-burst frequency range detected by FAST satellite wave receivers during overflights of the auroral zone; if associated with MF-burst, these observations and especially the simultaneous particle measurements available in the FAST data set may provide a breakthrough in understanding the MF-burst generation mechanism.

2.3. Auroral Hiss

The third type of spontaneous emission from the auroral ionosphere is auroral hiss. Auroral hiss was first reported over 70 years ago (Burton and Boardman, 1933), although it is controversial whether the initial observation was really auroral hiss rather than lightning-generated atmospherics (Morgan, 1977). Over this long length of time, a huge literature has developed on auroral hiss, and thorough reviews have been written by Makita (1979), Sazhin et al. (1993), and LaBelle and Treumann (2002). Ground-level observations of auroral hiss fall into two categories, impulsive hiss and continuous hiss. Continuous auroral hiss is long-duration but usually limited to VLF (below about 30 kHz). Impulsive auroral hiss usually lasts only a few minutes at substorm onsets but extends up as high as 1 MHz.

Figure 1 shows an example of impulsive auroral hiss occurring between 0652 and 0712 UT at frequencies up to 800 kHz. The coincidence with auroral MF-burst is stiking in this example as noted above. As with the MF-burst, the impulsive auroral hiss is associated with substorm onset which in this example occurs at 0652 UT. The power spectral density of impulsive auroral hiss typically peaks at VLF and decreases monotonically with frequency until the emission blends into the noise level at $\leq$ 1 MHz. The power spectral density at LF is of order 10^{-12} v^2/m^2Hz, comparable to that of auroral roar and MF-burst. On some occasions, only the LF component of auroral hiss is detected (Morgan, 1977; LaBelle et al., 1998).

As noted above, the whistler mode is characterized by a resonance cone for which the index of refraction greatly exceeds unity. Hence the non-relativistic 1-10 keV auroral electrons can resonate with these waves. The generally accepted generation mechanism for auroral hiss is coherent amplification of the whistler mode waves on the resonance cone via Landau resonance with the auroral electrons. Maggs (1976) presented the first detailed calculations of auroral hiss spectra from this mechanism. Convection of the waves away from the resonance condition with the auroral electrons significantly affects their amplification, and therefore the geometry and other characteristics of the auroral arc play a big role in determining the auroral hiss spectrum. At low frequencies, the ray direction of whistler modes on the resonance cone is roughly parallel to the magnetic field, so the waves move fairly rapidly out of resonance with the electron beam; at high frequencies, the ray direction of the resonance cone waves is roughly perpendicular to the magnetic field, so the waves spend a longer time at a given altitude but they may move out of the auroral arc which is limited in extent, especially in the north-south direction. Strong refraction of these waves out of the auroral arc limits their growth. Combining these effects in a realistic auroral arc model, Maggs (1976, 1978) predicts auroral hiss spectra that peak at VLF and decrease monotonically with frequency at LF. Furthermore, the power spectral densities predicted by the theory are comparable to those observed with satellites and rockets and, accounting for attenuation, at ground-level. Because of this striking quantitative agreement, the convective beam amplification (CBA) mechanism has become broadly accepted as the source of auroral hiss. Subsequent rocket measurements have confirmed the theory in some cases (e.g., Bering et al., 1987).

Despite the success of the CBA model, several features of auroral hiss remain mysterious. For example, propagation of auroral hiss from ionospheric sources to ground-level has never been fully explained. In order to reach ground-level, the waves must convert from whistler mode to free-space mode at the bottom of the ionosphere (called the Earth-ionosphere boundary). At VLF, this boundary may be treated as sharp. Because the whistler mode index of refraction greatly exceeds unity while that of the free-space mode equals

unity, the waves in effect impinge on the boundary from the high index of refraction side, so unless their wave vector is nearly perpendicular to the boundary, or vertical in this case, they are totally internally reflected and do not reach ground-level. The problem is, it is difficult to generate waves on the whistler mode resonance cone at ionopsheric altitudes and have them propagate to the Earth-ionosphere boundary with their wave-vector perpendicular. Matsuo et al. (1998) calculate that such propagation cannot happen in a slab mode ionosphere but claim that it can occur if horizontal gradients are included such as field-aligned ducts or a plasmapause gradient. However, Sonwalkar and Harikumar (2000) argue that Matsuo et al. (1998) achieve this result by starting the waves with their wave-vector unrealistically far off of the resonance cone. They suggest that if the waves start sufficiently close to the resonance cone to be excited by 1-10 keV auroral electrons, those waves cannot be sufficiently refracted to reach the Earth-ionosphere boundary with vertical wave vector, even if realistic horizontal gradients are included. Sonwalkar and Harikumar (2000) put forward a model whereby the whistler waves are scattered from much smaller scale density gradients such as those associated with meter-scale irregularities which are abundant in the auroral ionosphere. Through such scattering the whistler modes near the resonance cone can be promptly converted to whistler modes well off of the resonance cone, including waves that can reach the Earth-ionosphere boundary with near-vertical wave vectors. Interestingly, despite ground-level observations of auroral hiss going back 70 years, how the auroral hiss reaches ground level remains a controversial issue.

Figure 4 shows examples of high resolution spectra of auroral waves. The top panel represents ground-level measurements of magnetic field at frequencies up to 200 kHz recorded at South Pole, Antarctica; 5 s of data are shown. The bottom two panels represent rocket-borne measurements of electric field from two different experiments launched from Poker Flat, Alaska. The ground-based data (top panel) show the typical LF auroral hiss which consists of signals whose power spectral density peaks at VLF, below the receiver's range, and extends into the LF range with power spectral density decreasing with frequency. The spectrum is broadband and featureless as is considered typical for auroral hiss, which is so-named because the VLF (audio frequency) component usually sounds like a featureless "hiss" when played through a loudspeaker. This broadband hiss is well-described by calculations using CBA theory (e.g., Maggs, 1976, 1978). However, superposed on the broadband hiss in Figure 4 are discrete features which stand out from the background hiss. These features consist of multiple spectral lines with bandwidth of order 10 kHz superficially resembling the fine structure of auroral roar shown in Figure 3. Remarkably, these 20–40 kHz features stand out despite the high-pass filter which severely attenuates the background broadband auroral hiss. The power spectral density of these discrete features

exceeds that of the broadband auroral hiss by up to 40 dB, although its total power is comparable since its bandwidth is smaller by about the same factor. Similar fine structure of auroral hiss has been reported at VLF (Ungstrup, 1971), and at both VLF and LF other types of fine structures have been reported in ground-level data (e.g., Siren, 1975; Ye and LaBelle, 2005). So far no theory predicts such highly peaked spectra with such high power spectral density, though it cannot be excluded that the CBA theory might predict such spectra for the right combination of plausible auroral arc geometry and electron distribution functions.

The bottom panels of Figure 4 show two types of structured whistler mode waves observed at rocket altitudes. The middle panel shows two seconds of data from the SIERRA rocket experiment, launched January 14, 2002, from Alaska. The spectrogram spans 250–650 kHz. Broadband auroral hiss appears intermittently, extending from below 250 kHz to about 450 kHz. However, imbedded within it are dramatic fine structures which dominate the spectrogram. These include "stripes": multiple narrow-band features which decrease in frequency from about 500 kHz to about 250 kHz during about 0.5 seconds, and which have power spectral density comparable to the background broadband hiss but bandwidth of order 10 kHz (Samara and LaBelle, unpublished manuscript, 2006). More intense, impulsive patchy features occur at 370–570 kHz with bandwidth of order 100 kHz and power spectral density 10–20 dB higher than the broadband auroral hiss or the stripes. The bottom panel of Figure 4 shows five seconds of data from the PHAZE-II rocket experiment, launched February 10, 1997, from Alaska. The spectrogram spans 200–600 kHz and shows a different type of whistler mode fine structure which occurs when $f_{pe} < f_{ce}$: long-duration, constant-frequency "bands" with 10–20 kHz bandwidth and millivolt per meter amplitudes (McAdams et al., 1999). These signals last up to 30 s of the rocket flight, corresponding to about 30 km of altitude, and they are often punctuated by intense Langmuir waves where their frequencies match the local plasma frequency. McAdams et al. (1999) interpret them as signatures of intermittent intense Langmuir waves which mode convert to whistler mode in the region where $f_{pe} < f_{ce}$. Previous lower-resolution rocket and satellite experiments detected hints of this zoo of fine structures within auroral hiss (e.g., LaBelle et al., 1999; Shutte et al., 1997; Beghin et al., 1989). The frequency range and some of the characteristics of these fine structures correspond to those observed at much higher altitudes in Auroral Kilometric Radiation (AKR), and Oya et al. (1985) put forth that AKR, which normally propagates upward from sources at ~ 5000 kilometers altitude, can under some conditions couple to the whistler mode and propagate to ionospheric altitudes. If so, such "leaked AKR" could explain these fine structure observations and possibly some of those detected at ground level. However, this hypothesis has not been confirmed by other theoretical or observational studies and remains highly controversial.

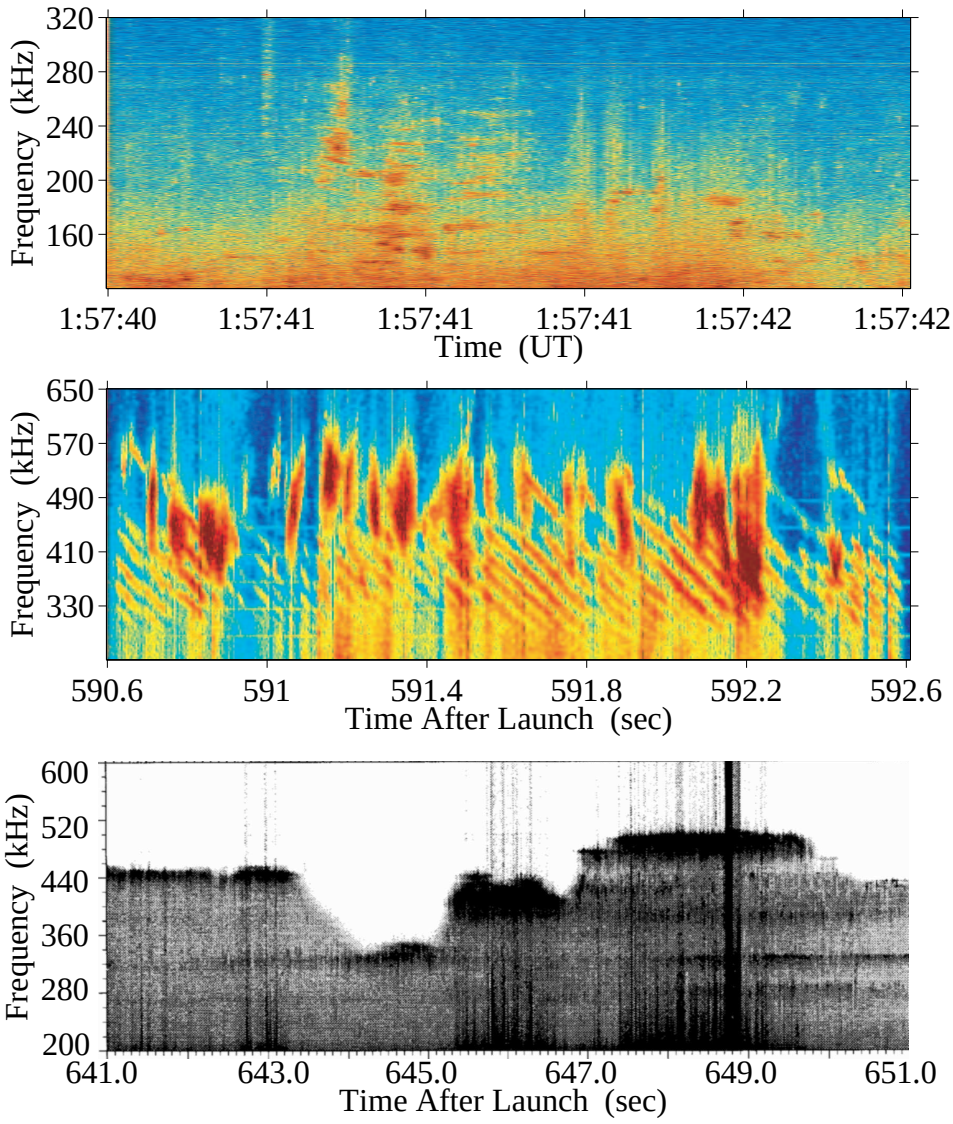

Figure 4. Fine structures characterizing whistler mode waves in the auroral ionosphere: (a) 120–320 kHz spectrogram of magnetic field fluctuations measured at ground-level at South Pole (2 s of data shown); (b) 250–650 kHz spectrogram of electric field fluctuations measured with the SIERRA rocket in Alaska (2 s of data shown); and (c) 200-600 kHz spectrogram of electric field fluctuations measured with the PHAZE-II rocket in Alaska (5 s of data shown). Different types of discrete features occur imbedded within the usual broadband auroral hiss.

In summary, impulsive auroral hiss, which occurs at substorm onset, often consists of a broadband spectrum of waves extending from VLF up to 1 MHz. Both the spectral shape and amplitude of this broadband hiss is well predicted by the CBA mechanism using reasonable models of the auroral electron distribution function and auroral arc. However, how these signals reach ground level remains controversial. At times various types of discrete whistler mode signals are imbedded in the broadband background auroral hiss, sometimes with power spectral densities greatly exceeding those of the background hiss. The origin of these signals is controversial. Despite 70 years of observations, auroral hiss is far from fully understood. Far more details of auroral hiss observations and theory can be found in comprehensive reviews (e.g., Sazhin et al., 1993; LaBelle and Treumann, 2002).

3. Summary

The discussion above focusses on three types of spontaneous emissions from the auroral ionosphere at radio frequencies: Auroral hiss, MF-burst, and roar, all of which can be observed at ground-level. Ground-level auroral roar occurs continuously for long durations, sometimes hours, preceding auroral substorms but becomes intermittent or absent after substorm onset, presumably due to poor propagation conditions which prevent the emission from reaching ground level. Impulsive auroral hiss and MF-burst are observed only for a few minutes at substorm onsets, presumably because the source conditions operate then but not at other times, and despite the relatively poor propagation conditions characterizing substorm onset. Auroral roar contains fine frequency structures which may carry information about ionospheric density irregularities. Auroral hiss and MF-burst may prove useful for timing and location of substorm onsets. Auroral hiss includes fine structures whose origin is not understood.

These three emissions are all relatively low-power in comparison with Auroral Kilometric Radiation (AKR). However, AKR cannot be considered an ionospheric emission because it is generated well above the ionosphere at thousands of kilometers altitude and beamed upward away from the ionosphere. Nevertheless, there are similarities between AKR and the lower altitude ionospheric radio emissions. The mechanism for most AKR is believed to be the X-mode cyclotron maser mechanism acting where the AKR frequency matches the local electron gyrofrequency, at altitudes of several thousand kilometers. This mechanism is similar to the Z-mode maser mechanism put forth to explain auroral roar emissions at F-region altitudes, except that in the AKR case the electrons directly excite the escaping X-mode and the radiated power is enormously greater. AKR exhibits fine structures which superficially resemble those which characterize auroral roar, but the mechanism

is unlikely to be the same since the modes are different. Calvert (1982) put forth a model for AKR fine structure that involved a wave feedback path with the wave path being an integer multiple of wavelengths, caused for example by reflection of the X-mode waves generated by the maser mechanism from reflection surfaces which converge with altitude (to compensate for refraction of the X-mode waves within the source region). Analogous to an optical laser, as long as the net gain around the feedback loop exceeds unity, the waves would grow to saturation with a tiny bandwidth, essentially monochromatic. In this model, many such compact radiators provide the source of the many narrow-band fine structures composing AKR. Observations of extremely narrow bandwidth AKR structures, of order 1 Hz, support this mechanism (Baumback and Calvert, 1987), but direct evidence is lacking. Recently, Mutel et al. (2005) propose an alternative model for one particular type of AKR fine structure, striated AKR, which consists of multiple descending tones. They put forth that the electric fields associated with ion phase space holes, features known to exist in the auroral acceleration region where AKR originates, locally distort the electron distribution function in such a way as to modulate the emission of AKR via the X-mode maser mechanism. Quantitative modelling shows that the modulation and frequency slope predicted by the theory agree quantitatively with those observed in striated AKR. Recently Bhesso et al. (2006) and Menietti et al. (2006) have explored variations of this model involving electromagnetic ion cyclotron waves rather than ion holes as the causative agent. Over the years, other mechanisms have been put forward to explain AKR fine structure (e.g., Louarn and Le Quéau, 1996a,b; Yoon and Weatherwax, 1998), but despite the success of certain models explaining subsets of the AKR fine structure, it remains an open problem.

The spontaneous auroral emissions also bear close similarities to stimulated electromagnetic emissions (SEE) generated by injection of high-power radio waves into the ionosphere (Thidé et al., 1982). A zoo of such emissions has been identified associated with different pump frequencies and powers (see review by Leyser, 2001). Some of these stimulated emissions closely resemble the natural spontaneous auroral emissions; in the one case the energy source is the injected pump wave, and in the other case, the auroral electrons.

The interconnections to other phenomena such as SEE and AKR provide a strong motivation for further investigation of the spontaneous emissions from the auroral ionosphere: not only are these an interesting component of Earth's radio environment which potentially play a significant role in that environment by interacting with particle populations and with other wave modes and which may serve as a useful ground-based diagnostic of ionospheric plasma processes, but understanding these auroral emissions originating a few hundred kilometers from Earth aids understanding of stimulated and spontaneous radio emission processes in a variety of other plasmas including other plane-

tary ionospheres and the solar wind. In some of these other cases, inaccessible to rocket and satellite experiments, the radio emissions are the primary means of sensing remote plasma processes.

Acknowledgements

The author thanks Shengyi Ye and Marilia Samara for help preparing the figures. The preparation of this review at Dartmouth College was partly supported by NASA grants NNG04WC27G, NNG05GM37G, and NNG05WC44G, and NSF grants ATM-0243595, ANT-0442369, and ANT-0341050.

References

Bale, S. D.: 1999, 'Observation of the topside ionospheric MF/HF radio emission from space'. *Geophys. Res. Lett.* **26**, 667.

Baumback, M. M. and W. Calvert: 1987, 'The minimum bandwidths of auroral kilometric radiation'. *Geophys. Res. Lett.* **14**, 119.

Beghin, C., J. L. Rauch, and J. M. Bosqued: 1989, 'Electrostatic Plasma Waves and HF Auroral Hiss Generated at Low Altitude'. *J. Geophys. Res.* **94**, 1359.

Bell, T. F. and H. D. Ngo: 1990, 'Electrostatic lower hybrid waves excited by electromagnetic whistler mode waves scattering from planar magnetic field aligned plasma density irregularities'. *J. Geophys. Res.* **95**, 149.

Benson, R. F. and H. K. Wong: 1987, 'Low-altitude ISIS 1 observations of auroral radio emissions and their significance to the cyclotron maser instability'. *J. Geophys. Res.* **92**, 1218.

Bering, E. A., J. E. Maggs, and H. R. Anderson: 1987, 'The Plasma Wave Environment of and Auroral Arc'. *J. Geophys. Res.* **92**, 7581.

Bhesso, N., D. Menietti, and A. Bhattacharjee: 2006, 'PIC Simulations of the Generation of Striated AKR'. *EOS Trans. Am. Geophys. Union* **87**(36), SM33B–03.

Burchill, J. K. and R. F. Pfaff: 2005, 'FAST observations of auroral MF emissions and precipitating electrons'. *EOS Trans. Am. Geophys. Union* **86**(52), SM44A–01.

Burton, E. T. and E. M. Boardman: 1933, 'Audio-frequency atmospherics'. *Proc. Inst. Radio Eng.* **21**, 1476.

Calvert, W.: 1982, 'A feedback model for the source of auroral kilometric radiation'. *J. Geophys. Res.* **87**, 8199.

Chiu, Y. T. and M. Schulz: 1978, 'Self-consistent particle and parallel electrostatic field distributions in the magnetospheric-ionospheric auroral zone'. *J. Geophys. Res.* **83**, 629.

Gough, M. P. and A. Urban: 1983, 'Auroral Beam/Plasma Interaction Observed Directly'. *Planet. Space Sci.* **31**, 875.

Hughes, J. M. and J. LaBelle: 1998, 'The latitude dependence of auroral roar'. *J. Geophys. Res.* **103**, 14911.

Hughes, J. M. and J. LaBelle: 2001a, 'First observations of flickering auroral roar'. *Geophys. Res. Lett.* **28**, 123.

Hughes, J. M. and J. LaBelle: 2001b, 'Plasma conditions in auroral roar source regions inferred from radio and radar observations'. *J. Geophys. Res.* **106**, 21157.

James, H. G., E. L. Hagg, and L. P. Strange: 1974, 'Narrowband radio noise in the topside ionosphere'. *AGARD Conf. Proc.* **AGARD-CP-138**, 24–1–24–7.

Kaufmann, R. L.: 1980, 'Electrostatic wave growth: secondary peaks in measured auroral electron distribution functions'. *J. Geophys. Res.* **85**, 1713.

Kellogg, P. J. and S. J. Monson: 1979, 'Radio emissions from the aurora'. *Geophys. Res. Lett.* **6**, 297–300.

LaBelle, J., K. L. McAdams, and M. L. Trimpi: 1999, 'High-frequency and time resolution rocket observations of structured low- and medium-frequency whistler mode emissions in the auroral ionosphere'. *J. Geophys. Res.* **104**, 28,101.

LaBelle, J., S. G. Shepherd, and M. L. Trimpi: 1997, 'Observations of auroral medium frequency bursts'. *J. Geophys. Res.* **102**, 22,221.

LaBelle, J. and R. A. Treumann: 2002, 'Auroral Radio Emissions, 1. Hisses, Roars, and Bursts'. *Space Sci. Rev.* **99**, 295–440.

LaBelle, J., M. L. Trimpi, R. Brittain, and A. T. Weatherwax: 1995, 'Fine structure of auroral roar emissions'. *J. Geophys. Res.* **100**, 21953.

LaBelle, J., A. T. Weatherwax, J. Perring, E. Walsh, M. L. Trimpi, and U. Inan: 1998, 'Low-frequency impulsive auroral hiss observations at high geomagnetic latitudes'. *J. Geophys. Res.* **103**, 20459–20468.

Leyser, T. B.: 2001, 'Stimulated electromagnetic emissions by high-frequency electromagnetic pumping of the ionospheric plasma'. *Space Sci. Rev.* **98**, 223 – 328.

Louarn, P. and D. Le Qu´eau: 1996a, 'Generation of auroral kilometric radiation in plasma cavities, I, Experimental study'. *Planet. Space Sci.* **44**, 199.

Louarn, P. and D. Le Qu´eau: 1996b, 'Generation of auroral kilometric radiation in plasma cavities, II, The cyclotron maser instability in small size sources'. *Planet. Space Sci.* **44**, 211.

Maggs, J. E.: 1976, 'Coherent Generation of VLF Hiss'. *J. Geophys. Res.* **81**, 1707.

Maggs, J. E.: 1978, 'Electrostatic Noise Generated by the Auroral Electron Beam'. *J. Geophys. Res.* **83**, 3173.

Makita, K.: 1979, 'VLF/LF hiss emissions associated with aurora'. *Mem. Nat. Int. Polar Res.* **16**, 1.

Matsuo, T., T. Nishiyama, and D. Matuhara: 1998, 'Propagation of a quasi electrostatic whistler mode auroral hiss to the ground'. *Proc. NIPR Symp. Upper Atmos. Phys.* **12**, 12–29.

McAdams, K. L., J. LaBelle, M. L. Trimpi, P. M. Kintner, and R. A. Arnoldy: 1999, 'Rocket observations of banded stucture in waves near the Langmuir frequency in the auroral ionosphere'. *J. Geophys. Res.* **104**, 28109.

Menietti, J. D., R. L. Mutel, O. Santolik, J. D. Scudder, I. W. Christopher, and J. M. Cook: 2006, 'Striated drifting auroral kilometric radiation bursts: Possible stimulation by upward traveling EMIC waves'. *J. Geophys. Res.* **111**, A04214, doi:10.1029/2005JA011339.

Morgan, M. G.: 1977, 'Wide-Band Observations of LF Hiss at Frobisher Bay ($L = 14.6$)'. *J. Geophys. Res.* **82**, 2377.

Mutel, R. L., D. Menietti, and I. Christopher: 2005, 'Striated AKR: A Remote Tracer of Solitary Ion Structures in the Magnetosphere'. *EOS Trans. Am. Geophys. Union* **86**(52), SM41B–1189.

Oya, H., A. Morioka, and T. Obara: 1985, 'Leaked AKR and Terrestrial Hectometric Radiations Discovered by the Plasma Wave and Planetary Plasma Sounder Experiments on Board the Ohzora (EXOS-C) Satellite- Instrumentation and Observation Results of Plasma Wave Phenomena'. *Geomag. Geoelectr.* **37**, 237.

Parthasarathy, R. and F. T. Berkey: 1964, 'Radio noise from the auroral electrons-I'. *J. Atmos. Terr. Phys.* **26**, 199.

Samara, M., J. LaBelle, C. A. Kletzing, and S. R. Bounds: 2004, 'Rocket observations of structured upper hybrid waves at $f_{uh} = 2f_{ce}$'. *Geophys. Res. Lett.* **31**(L22804), doi:10.1029/2004GL021043.

Sazhin, S. S., K. Bullough, and M. Hayakawa: 1993, 'Auroral hiss: A review'. *Planet. Space Sci.* **41**, 153–166.

Shepherd, S. G., J. LaBelle, and M. L. Trimpi: 1997, 'The polarization of auroral radio emissions'. *Geophys. Res. Lett.* **24**, 3161.

Shepherd, S. G., J. LaBelle, and M. L. Trimpi: 1998, 'Further investigation of auroral roar fine structure'. *J. Geophys. Res.* **103**, 2219.

Shutte, N., I. Prutensky, S. Pulinets, Z. Klos, and H. Rothkaehl: 1997, 'The charged-particle fluxes at auroral and polar latitudes and related low-frequency auroral kilometric radiation-type and high-frequency wideband emission'. *J. Geophys. Res.* **102**, 2105.

Siren, J. C.: 1975, 'Fast Hisslers in Substorms'. *J. Geophys. Res.* **80**, 93.

Sonwalkar, V. S. and J. Harikumar: 2000, 'An explanation of ground observations of auroral hiss: Role of density depletions and meter scale irregularities'. *J. Geophys. Res.* **105**, 18867–18883.

Sotnikov, V. I., D. Schriver, M. Ashour-Abdalla, and J. LaBelle: 1996, 'Generation of auroral radio waves by a gyrating electron beam'. *EOS Trans. Am. Geophys. Union* **77**, F544.

Thid´e, B., H. Kopka, and P. Stubbe: 1982, 'Observations of Stimulated Scattering of a Strong High Frequency Radio Wave in the Ionosphere'. *Phys. Rev. Lett.* **49**, 1561–1564.

Ungstrup, E.: 1971, 'Rocket Observation of VLF Hiss in Aurora'. *Planet. Space Sci.* **19**, 1475.

Weatherwax, A. T., J. LaBelle, and M. L. Trimpi: 1994, 'A new type of auroral radio emission observed at medium frequencies($\sim 1350 - 3700$ kHz) using ground-based receivers'. *Geophys. Res. Lett.* **21**, 2753.

Weatherwax, A. T., J. LaBelle, M. L. Trimpi, and R. Brittain: 1993, 'Ground-based observations of radio emissions near $2f_{ce}$ and $3f_{ce}$ in the auroral zone'. *Geophys. Res. Lett.* **20**, 1447–1450.

Weatherwax, A. T., J. LaBelle, M. L. Trimpi, R. A. Treumann, J. Minow, and C. Deehr: 1995, 'Statistical and case studies of radio emissions observed near $2f_{ce}$ and $3f_{ce}$ in the auroral zone'. *J. Geophys. Res.* **100**, 7745.

Ye, S. and J. LaBelle: 2005, 'High Resolution Measurement of LF Auroral Hiss at South Pole'. *EOS Trans. Am. Geophys. Union* **86**(18), SM43C–07.

Yoon, P. H. and A. T. Weatherwax: 1998, 'Theory for AKR fine frequency structure'. *Geophys. Res. Lett.* **25**, 4461–4464.

Yoon, P. H., A. T. Weatherwax, and J. LaBelle: 2000, 'Discrete electrostatic eigenmodes associated with ionospheric density structure: Generation of auroral roar fine frequency structure'. *J. Geophys. Res.* **105**, 27589.

Yoon, P. H., A. T. Weatherwax, and T. J. Rosenberg: 1996, 'Lower ionospheric cyclotron maser theory: A possible source of 2fce and 3fce auroral radio emissions'. *J. Geophys. Res.* **101**, 27,015.

Yoon, P. H., A. T. Weatherwax, and T. J. Rosenberg: 1998a, 'On the generation of auroral radio emissions at harmonics of the lower ionospheric electron cyclotron frequency: X, O and Z Mode maser calculations'. *J. Geophys. Res.* **103**, 4071.

Yoon, P. H., A. T. Weatherwax, T. J. Rosenberg, J. LaBelle, and S. G. Shepherd: 1998b, 'Propagation of medium frequency (1-4 MHz) auroral radio waves to the ground via the Z-Mode radio window'. *J. Geophys. Res.* **103**, 29267.